Available online at www.sciencedirect.com

SciVerse ScienceDirect

Ceramics International 39 (2013) 8347–8354

CERAMICS INTERNATIONAL

www.elsevier.com/locate/ceramint

Solvothermal growth of three-dimensional TiO_2 nanostructures and their optical and photocatalytic properties

Jing Zhou[a,b], Gaoling Zhao[a,*], Gaorong Han[a], Bin Song[c]

[a]State Key Laboratory of Silicon Materials and Department of Materials Science and Engineering, Zhejiang University, Hangzhou 310027, PR China

[b]Zhejiang Police College, Hangzhou 310053, PR China

[c]Department of Physics, Zhejiang University, Hangzhou 310027, PR China

Received 15 March 2013; received in revised form 22 March 2013; accepted 28 March 2013
Available online 11 April 2013

Abstract

Three-dimensional (3D) titania nanostructures assembled with ordered rutile nanorods have been fabricated via a surfactant-free and single-step solvothermal route. The effects of preparation parameters, including the reaction temperatures and the reactant concentrations, on the microstructure, optical properties and photocatalytic activity of the 3D TiO_2 nanostructures were investigated. The results revealed that 3D TiO_2 microspheres possessed a dandelion-like morphology composed of radially packed rutile nanorods. Increasing the reaction temperature leads to the formation of larger rutile crystals, but reduced the aspect ratios of nanorods. The morphology of products was dominated by irregular shapes with low titanium precursor concentration. The optical reflectance, absorption and photocatalytic properties of the samples were found to be significantly dependent on their morphology. 3D dandelion-like structures with tapered tips showed lower reflectance, more efficient light harvesting, higher surface area and consequently higher photocatalytic activity compared with those with flat tops and fragment of nanorod sectors. Moreover, TiO_2 products prepared with 0.4 M titanium precursor solution at 150 and 120 °C showed better or equivalent photocatalytic activity compared with Degussa P25 owing to high light harvesting ability as well as less aggregation for the unique 3D dandelion-like hierarchical structure. The growth mechanism of the 3D dandelion-like nanostructures under various preparation conditions was also discussed.

Keywords: C. Optical properties; D. TiO_2; Nanostructures; Photocatalysis

1. Introduction

In recent decades, titanium dioxide (TiO_2) is widely used in diverse applications such as photocatalysts, dye-sensitized solar cells and biomedicines [1–4]. Therefore, considerable efforts have been paid to synthesize TiO_2 nanostructures. Studies have revealed that it is critical to control the morphology and crystal structures of nanostructure since the properties and performance such as optical and photocatalytic properties are greatly dependent on the microstructure, specific surface area and crystallite size [5–9]. Assembly of various TiO_2 nanometer-scale units into three-dimensional (3D) complex nanostructures has triggered considerable attention because of the dimension and unique topology [10]. This kind of 3D artificial hierarchical TiO_2 structures could reserve novel properties due to the nanometer-scale unit, meanwhile, they are much easier to store and handle as micrometer-scale materials [10]. For instance, microspheres assembled with nanorods are expected to exhibit low reflectance and efficient light harvesting due to the ordered nanorod units. Moreover, traditional TiO_2 nanometer-scale powders suffer from severe agglomeration, while 3D microscale TiO_2 nanostructures are less likely to aggregate and easier to be separated from the solution as photocatalyst. It might offer opportunities for fundamental study and industrial applications to explore 3D TiO_2 nanostructures under effective morphology control.

The solvothermal method is a simple, low-cost and highly efficient synthetic approach for nanostructures, and the process could be easily controlled [11,12]. Furthermore, it has been proven that the growth of semiconductor nanostructures as well as their properties significantly depends on the preparation process [6,13]. In our previous work, the solvent-controlled fabrication of 3D TiO_2 nanostructures has been achieved via a

*Corresponding author. Tel./fax: 86 571 87952341.
E-mail address: glzhao@zju.edu.cn (G. Zhao).

0272-8842/$ - see front matter © 2013 Elsevier Ltd and Techna Group S.r.l. All rights reserved.
http://dx.doi.org/10.1016/j.ceramint.2013.03.105

surfactant-free and single-step solvothermal route [14]. In this paper, TiO_2 microspheres assembled with ordered rutile nanorods were synthesized in nonpolar solvent based on the water–nonpolar solvent interface. The effects of various experimental parameters, including reaction temperatures and the reactant concentrations, on the microstructure and structure-dependent optical and photocatalytic properties were studied. The growth mechanism of 3D TiO_2 nanostructures under various preparation conditions was also discussed.

2. Experimental section

2.1. Preparation

The synthesis of TiO_2 samples was based on our previous report with some modifications [14]. All the chemicals were of analytic grade and used without further purification. Titanium *n*-butoxide ($Ti(OC_4H_9)_4$, TNB), hydrochloric acid (HCl, 36.5–38 wt%), and *n*-hexane ($CH_3(CH_2)_4CH_3$) were used as the titanium precursor, acid medium, and the solvent, respectively. In a typical synthesis, 0.4 M TNB and 0.9 M HCl were added to *n*-hexane in a total volume of 26 ml. The mixture was stirred for 10 min and finally loaded into a Teflon-lined autoclave of 50 ml capacity and tightly closed for the solvothermal reaction. Subsequently, the autoclave was maintained at 120–210 °C for 4 h, followed by natural cooling to room temperature. Afterward, the products were centrifuged and washed with absolute ethanol several times. The final products were dried under vacuum at 80 °C for 12 h. In order to investigate the effects of TNB concentration, the TNB concentration was tuned to 0.5 M, 0.3 M, and 0.2 M, respectively, at a reaction temperature of 180 °C, remaining all other procedures unchanged.

2.2. Characterization

The morphologies of TiO_2 samples were investigated by field emission scanning electron microscopy (FESEM, Hitachi S-4800, Japan) and transmission electron microscopy (TEM, Philips C200, Germany). The crystal phases of the products were characterized by X-ray diffraction (XRD, PANalytical X'Pert Pro, Holland), in a 2θ range from 10° to 80°, using Cu Kα radiation. The optical absorption measurement was performed on a UV–vis spectrophotometer (TU-1901, Puxi Ltd. of Beijing, China), and diffuse reflectance was measured using an integrating sphere with an incident angle of 8°. The Brunauer–Emmett–Teller (BET) surface areas of the powder samples were determined by nitrogen adsorption–desorption isotherm measurements at 77 K on a Micromeritics TriStar II 3020 nitrogen adsorption apparatus. All the samples were degassed at 180 °C prior to the nitrogen adsorption measurements.

2.3. Photocatalysis tests

The photocatalytic activity of TiO_2 samples were tested by degrading Rhodamine B (RhB) in an aqueous solution. In a typical procedure, 10 mg TiO_2 powder was dispersed in 10 mL RhB aqueous solution with an initial concentration of 10^{-5} M. This reaction dispersion was magnetically stirred in the dark for 60 min prior to irradiation to establish the adsorption/desorption equilibrium. The solution was then exposed to UV light (80 W xenon arc lamp with a 420 nm cut-off filter). The distance between the light source and the bottom of the solution was about 15 cm. After illumination, the TiO_2 powder was removed from the suspension by centrifugation before the absorption spectrum was taken by a UV–vis spectrophotometer. The photodegradation effect is studied by the absorbance at the absorption peak before and after photodegradation, since the concentration of RhB solution is correlated to the absorption value. The photocatalytic activity could be characterized by an apparent speed constant k, which could be calculated using the equation as follows:

$$k = \frac{ln(A_0/A)}{t} \quad (1)$$

where A_0 is the absorbance of the initial RhB solution at 553 nm and A is the absorbance of RhB at 553 nm when irradiation time is 5, 10, 15, and 20 min. The higher the value of k, the better the photocatalytic activity.

3. Results and discussion

3.1. Effects of reaction temperature on the microstructures of TiO_2

The XRD patterns of the as-prepared TiO_2 samples fabricated with a TBN concentration of 0.4 M at various reaction temperatures are shown in Fig. 1. All the characteristic peaks can be indexed as a rutile TiO_2 phase (JCPDS no. 21-1276). The diffraction peaks gradually become sharper and narrower with increasing reaction temperature, indicating the enhancement

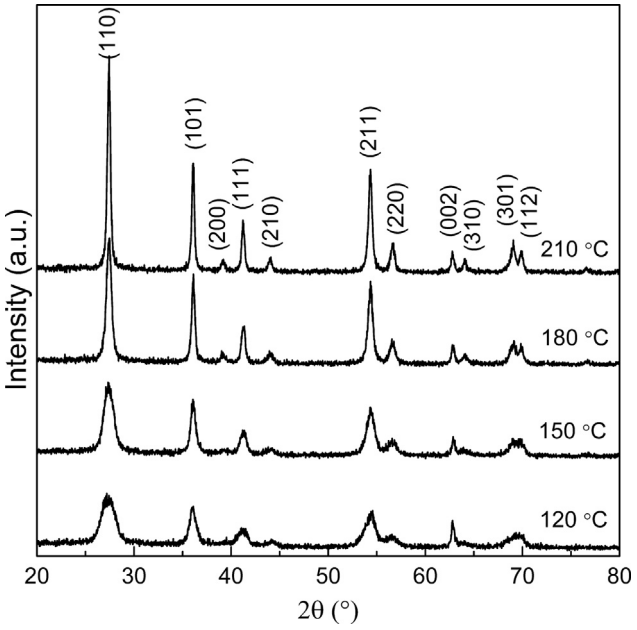

Fig. 1. XRD patterns of the products synthesized with a TBN concentration of 0.4 M at various reaction temperatures of 120, 150, 180, and 210 °C, respectively.

of crystallinity and growth of nanocrystals at higher reaction temperature.

Fig. 2 shows the typical FESEM images of the products synthesized with a TBN concentration of 0.4 M at various reaction temperatures. At 120 °C, the products have a dandelion-like structure with diameter of 1 μm, which is composed of numerous nanorods (Fig. 2a). Obviously, there are some crackles in the spheres. The average diameter of the nanorods is 5 nm as shown in Fig. 2b. Increasing the temperature to 150 °C and 180 °C, the size of the spheres and the diameter of nanorods rise to 1.5 μm and 10 nm at 150 °C (Fig. 2c and d), 2 μm and 18 nm at 180 °C (Fig. 2e and f), respectively. With the reaction temperature elevates to 210 °C, the nanorod density significantly increases, and the diameter of nanorods increases to 35 nm, as shown in Fig. 2g and h. The size of the spheres is in range of 1–2.5 μm. The aspect ratio of the nanorods for the samples prepared at 120, 150, 180, and 210 °C is 100, 75, 55, and 14–35, respectively. The results indicate that

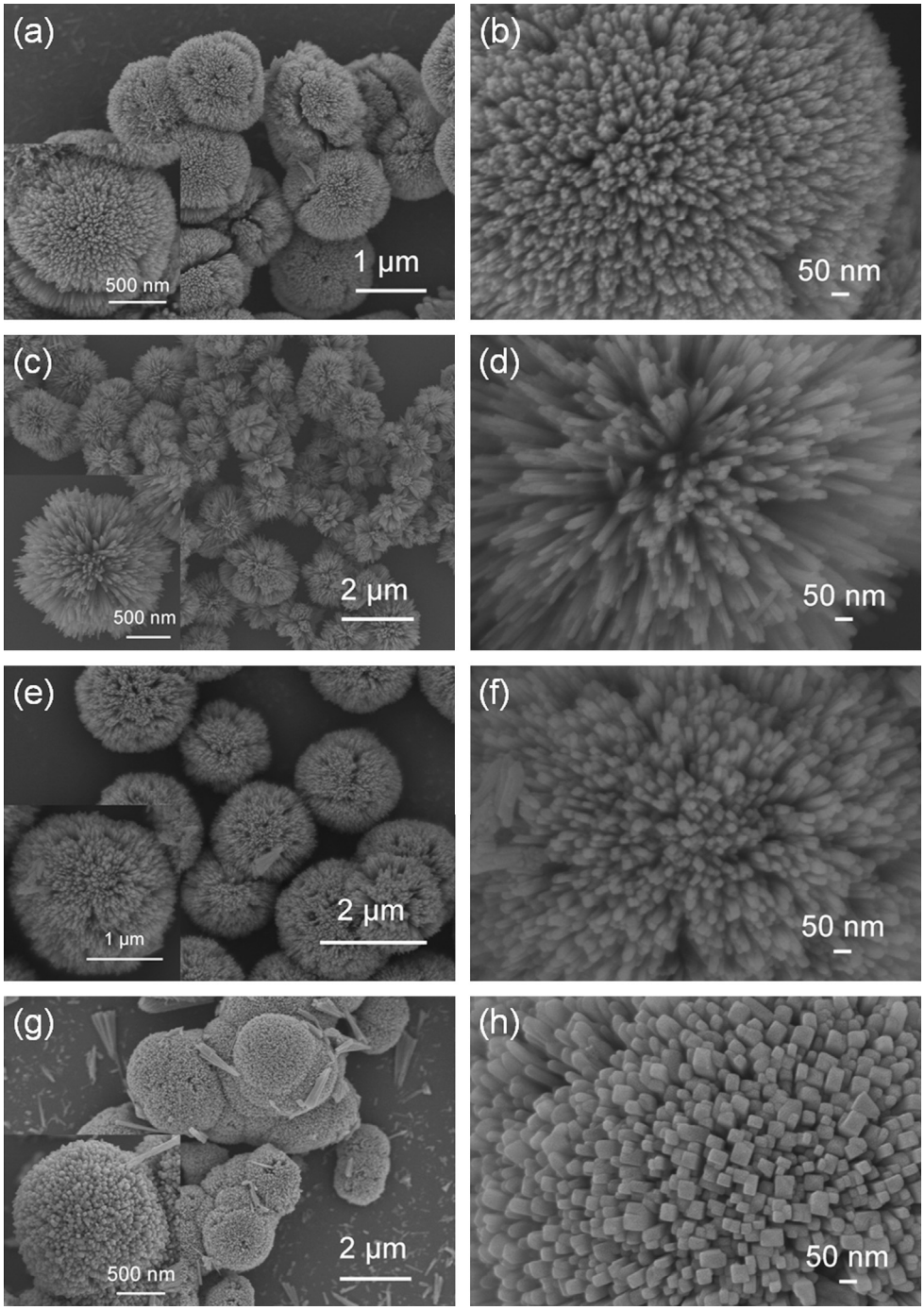

Fig. 2. Typical FESEM images of the products synthesized with a TBN concentration of 0.4 M at various reaction temperatures: (a, b) 120 °C, (c, d) 150 °C, (e, f) 180 °C, and (g, h) 210 °C. (a), (c), (e), and (g) are overview FESEM images. (b), (d), (f), and (h) are enlarged FESEM images of the surfaces of the corresponding samples.

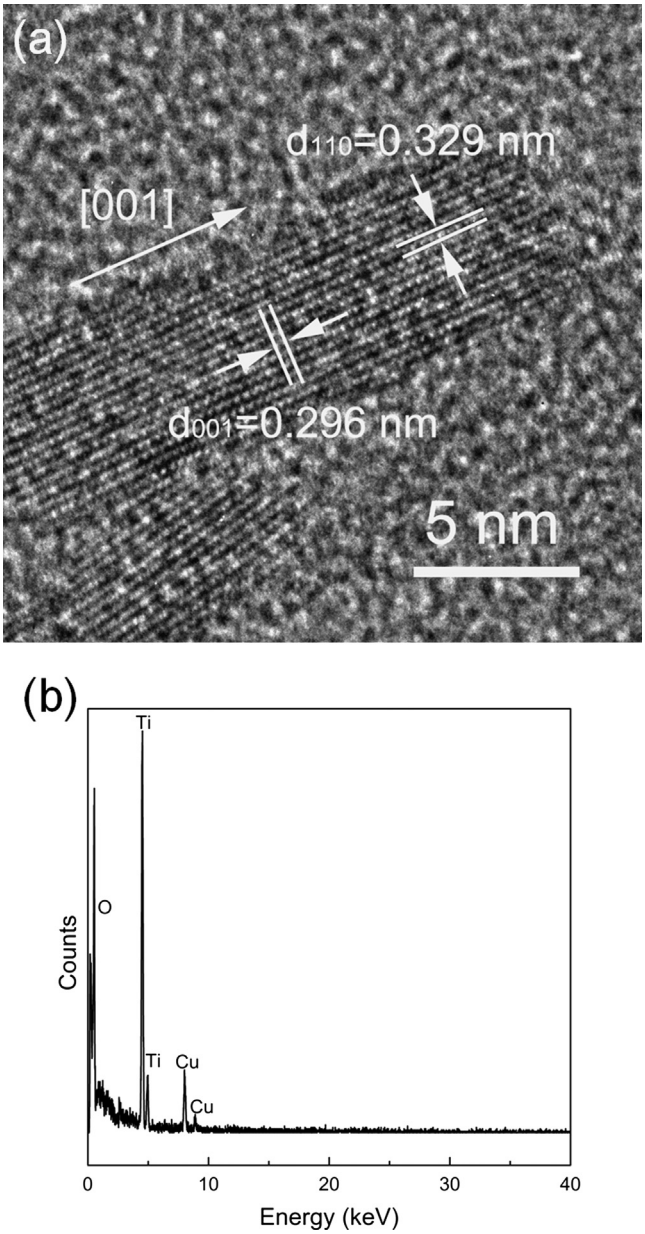

Fig. 3. (a) HRTEM image of an individual nanorod and (b) EDX profile of the dandelion-like structure synthesized with a TBN concentration of 0.4 M at 120 °C.

increasing the reaction temperature leads to the formation of larger nanorods and spheres, but reduces the aspect ratios of the one-dimensional nanocrystals.

HRTEM image of an individual nanorod and EDX profile of the dandelion-like structure synthesized with a TBN concentration of 0.4 M at 120 °C are shown in Fig. 3. The distances between the adjacent lattice fringes are measured to be 0.329 and 0.296 nm, which agree well with the lattice spacing of rutile TiO_2 (110) and (001) (JCPDS no. 21-1276), respectively, indicating the growth direction of [001], parallel to the *c*-axis. EDX spectrum reveals only Ti and O peaks in the sample with a Ti/O molar of about 1:2, and the Cu signal originates from the copper TEM grid. The EDX analysis confirms the purity and atomic composition of Ti and O in stoichiometric ratio.

3.2. Effects of TNB concentration on the microstructures of TiO_2

Besides the reaction temperature, the concentration of TNB is another influencing factor on the growth of TiO_2 microstructures. Fig. 4 shows XRD patterns of the products synthesized at 180 °C with TBN concentrations of 0.5 M, 0.3 M, and 0.2 M, respectively. All the peaks can be assigned to rutile TiO_2 (JCPDS no. 21-1276). It can be inferred from the weaker diffraction peaks that the crystallinity of crystals declines with lower TNB concentration.

Fig. 5 shows typical FESEM images of the products synthesized at 180 °C with various TBN concentrations. It can be seen that the products synthesized with TNB concentration of 0.5 and 0.3 M are dandelion-like microspheres. The average diameters of the microspheres and nanorods are 2 μm and 25 nm for 0.5 M TNB (Fig. 5a and b), 1 μm and 15 nm for 0.3 M TNB (Fig. 5c and d), respectively. The aspect ratios of the nanorods for the products fabricated with 0.5 and 0.3 M TNB concentration are 40 and 33, respectively. However, when the amount of TNB is as low as 0.2 M, the products are irregular sectors composed of nanorods (as shown in Fig. 5e and f) and there is no microsphere formed. The length of sectors and diameter of nanorods are 0.5–2 μm and 10 nm, respectively.

3.3. Growth mechanism of 3D TiO_2 nanostructures

From the kinetics viewpoint of crystal growth, the formation of rutile nanorod-aggregated objects is driven by low degree of supersaturation [15–17]. Generally, the condition is satisfied by using aqueous titanium trichloride precursor ($TiCl_3$) via the anodic oxidative hydrolysis of Ti (III) ions [10,15,18]. In the present case, the precursor used is Ti (IV) complex. The required low degree of supersaturation is achieved by the

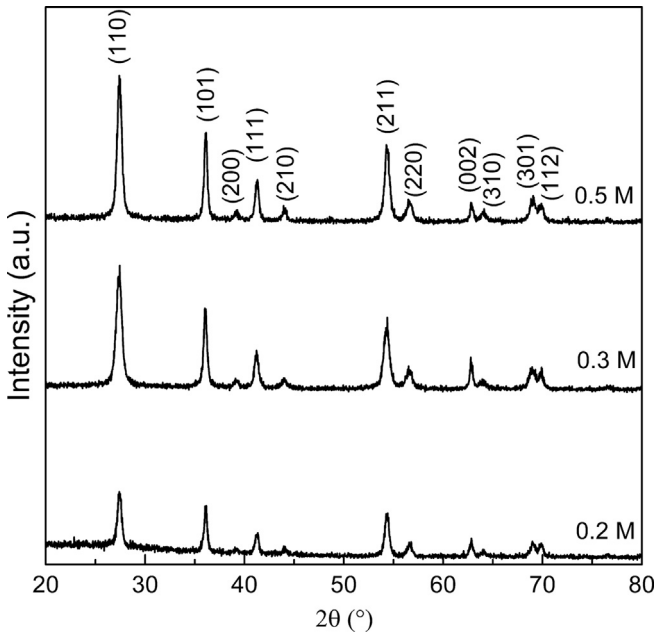

Fig. 4. XRD patterns of the products synthesized at 180 °C with various TBN concentrations: 0.5 M, 0.3 M, and 0.2 M.

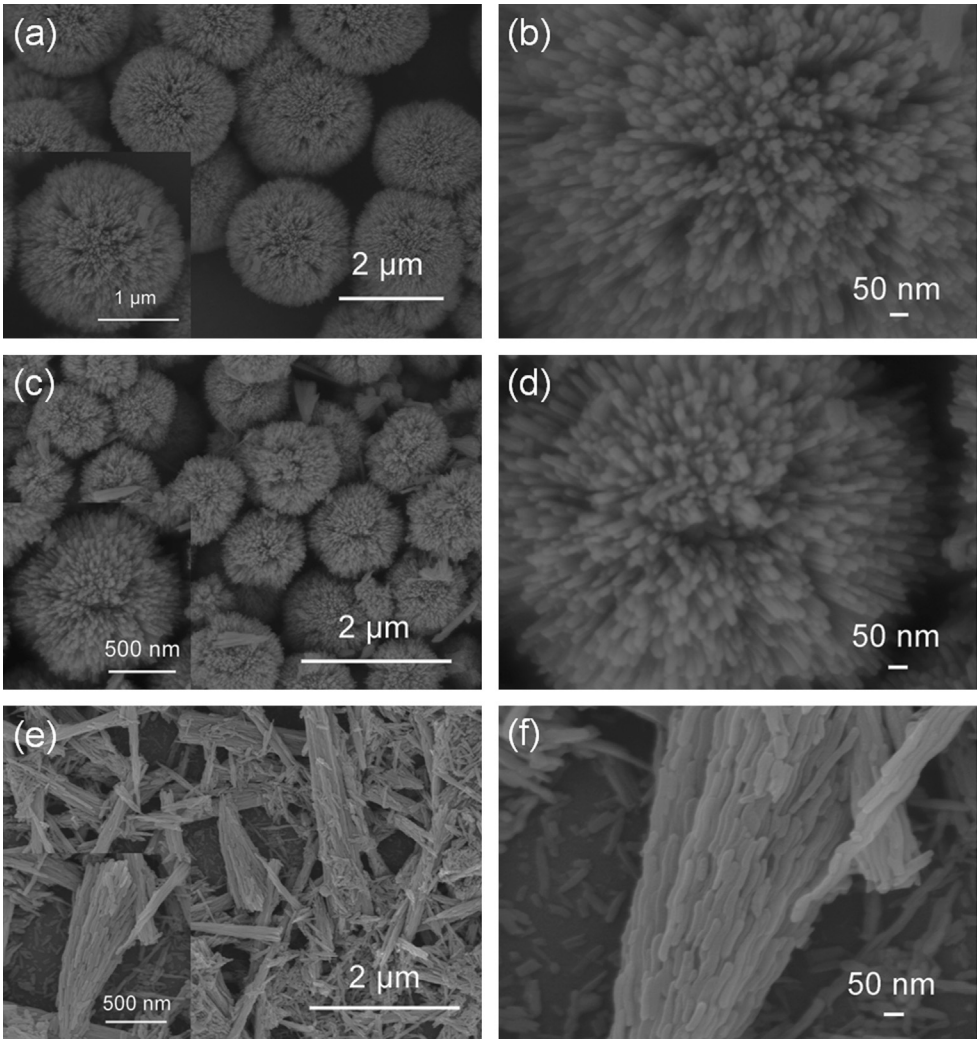

Fig. 5. Typical FESEM images of the products synthesized at 180 °C with various TBN concentrations: (a, b) 0.5 M, (c, d) 0.3 M, and (e, f) 0.2 M. (a), (c), and (e) are overview FESEM images. (b), (d), (f) are enlarged FESEM images of the surfaces of the corresponding samples.

existence of the acid medium HCl. The chemical reactions can be described as follows [17,19,20].

$$Ti^{4+} + nH_2O \rightarrow Ti(OH)_n^{4-n} + nH^+ \quad (2)$$

$$Ti(OH)_n^{4-n} \rightarrow Ti(IV)\ \text{oxo species} \rightarrow TiO_2 \quad (3)$$

The Ti (IV) oxo species are generally considered to be intermediates between TiO^{2+} and TiO_2, consisting of partly dehydrated polymeric Ti (IV) hydroxide [15,20]. The acid condition could retard the hydrolysis reaction of TNB (reaction (2)) by decomposing to free H^+, leading to a low degree of supersaturation which consequently slows the formation process of the intermediate Ti (IV) oxo species. Meanwhile, both the highly acid condition and selectively adsorption of Cl^- on rutile (110) plane facilitate the anisotropic growth of rutile nanorods along [001] orientation [21,22]. The nanorods aggregate into dandelion-like microspheres to lower their total free energy.

The growth mechanism of the 3D dandelion-like nanostructures under various experimental conditions is illustrated in Fig. 6. The low concentration of TNB (0.2 M) gives rise to a small amount of $Ti(OH)_n^{4-n}$, the hydrolysate of TNB. It enhances the preferred growth of longer rodlike rutile TiO_2 along the *c*-axis and the formation of sector-like nanostructure rather than dandelion-like microspheres due to the lower degree of supersaturation. However, with increasing concentration of TNB (0.3 M or higher), plenty of $Ti(OH)_n^{4-n}$ and consequently a large amount of TiO_2 nanorods are produced, causing the radial growth of 3D dandelion-like microspheres assembled with numerous oriented nanorods. Further increasing the concentration of TNB (0.5 M), the average diameter of the nanorods grows larger while the size of the microspheres remains almost the same, which can be ascribed to the block of oriented growth owing to the higher degree of supersaturation at higher TNB concentration. On the other hand, higher temperature accelerates the hydrolysis of TNB, resulting in not only larger number of TiO_2 nuclei but also faster crystal growth. It is noteworthy that larger rutile nanorods but lower aspect ratios are generated at higher temperature due to the accelerated growth in both radial and lengthwise directions.

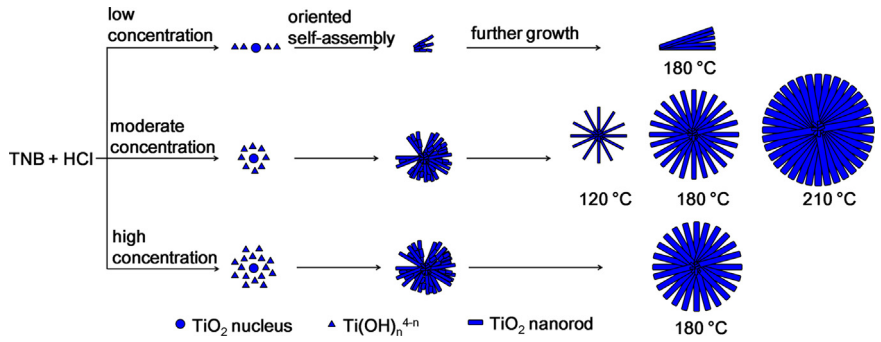

Fig. 6. Schematic illustrations of growth mechanism of the 3D dandelion-like nanostructures under various experimental conditions.

3.4. Optical and photocatalytic properties

The optical diffuse reflectance and absorption spectra of 3D TiO_2 structures synthesized under various conditions are shown in Fig. 7. As seen in Fig. 7a, the fast decay below 400 nm is due to the absorption of light caused by the excitation of electrons from the valence band to the conduction band of TiO_2, which correlates with the band gap of rutile TiO_2 (3.0 eV). The TiO_2 samples exhibit different reflectance on account of the difference in morphology. The samples prepared with 0.4 M TNB at 120 and 150 °C, and 0.3, 0.4, and 0.5 M TNB at 180 °C, which possess 3D dandelion-like structure with tapered tips show lower reflectance compared with those synthesized with 0.4 M TNB at 210 °C and 0.2 M TNB at 180 °C, which have flat tops and fragment of nanorod sectors. The interspaces between ordered rods can act as a light-transfer path for introducing incident light into the inner surface of TiO_2, allowing light waves to penetrate deep inside the TiO_2 structure. The multiple reflective and scattering effects provided by nanorods prevent the incident waves from bouncing back to the free space. Both of these lead to a lower reflection. The reflectance has been proven to be significantly dependent on the surface geometry [23–25]. Generally, tapered tips and moderate oriented rods are beneficial to low reflectance in comparison with flat tops and dense arrangement. Therefore, the increase in reflectance for TiO_2 prepared with 0.4 M TNB at 210 °C and 0.2 M TNB at 180 °C can be attributed to the flat tops and collapse of 3D dandelion-like structure. The optical absorption spectra shown in Fig. 7b indicate that all the samples have the absorption edge at around 400 nm, which is in agreement with the reflectance spectra. The absorption of the samples is in converse orders compared with the reflectance spectra. The sample prepared with 0.4 M TNB at 150 °C exhibits the lowest reflectance, most intense absorption and efficient light harvesting, due to its tapered tips and appropriately arrangement of nanorods in the 3D dandelion-like structure.

Fig. 8 shows the BET surface areas and plots of photocatalytic degradation of RhB using 3D TiO_2 nanostructures with different morphologies. TiO_2 dandelion-like structures prepared with 0.3–0.5 M TNB at 120–180 °C show higher BET surface areas than those prepared with lower TNB concentration or at higher reaction

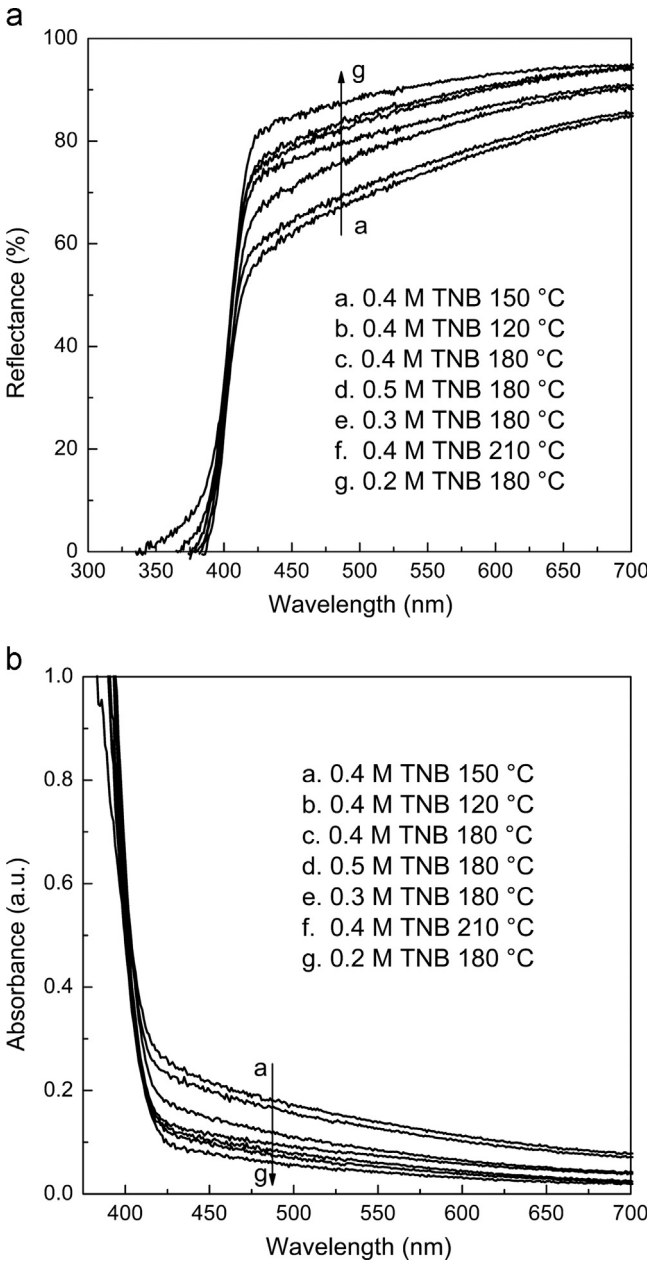

Fig. 7. (a) Optical diffuse reflection spectra and (b) absorption spectra of 3D TiO_2 nanostructures synthesized under various conditions.

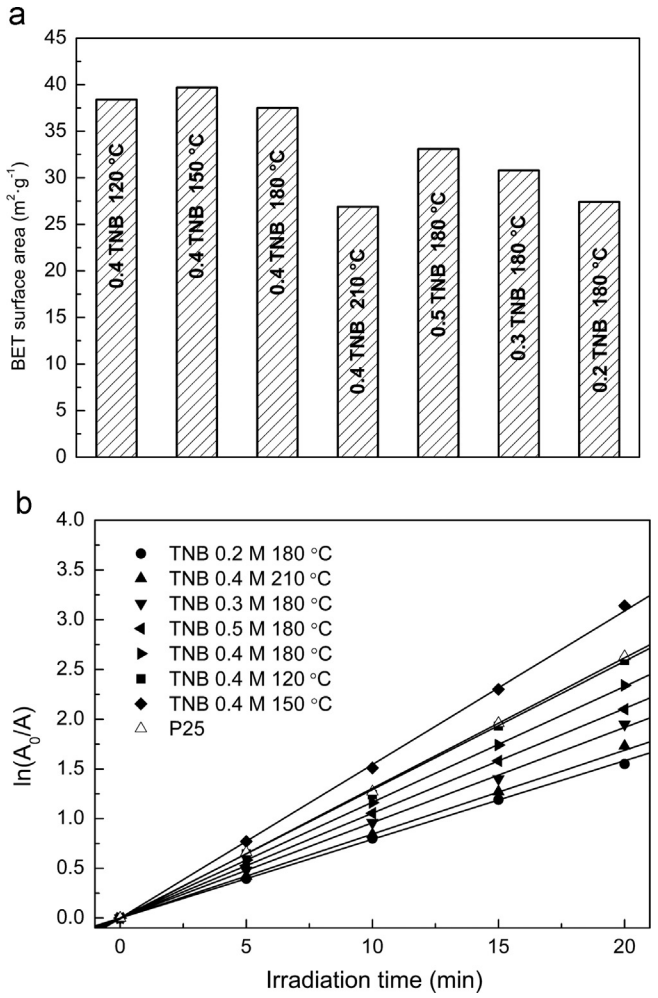

Fig. 8. (a) BET surface areas and (b) plots of photocatalytic degradation of RhB using 3D TiO_2 nanostructures synthesized under various conditions.

temperature due to the appropriate nanorod arrangement. Consequently, they exhibit higher degradation efficiency since high surface area provides more active sites to adsorb reactant molecules and tapered tip geometry allows more efficient utilization of incident light, both of which facilitate the enhancement of photocatalytic activity. The sample prepared with 0.2 M TNB at 180 °C, possessing the morphology of sectors, exhibits the lowest degradation efficiency. This can be explained by the collapse of 3D dandelion-like architecture, leading to much more severe aggregation and lower surface area as well as low light harvesting.

For comparison, Degussa P25 is also used as the photocatalyst, as shown in Fig. 8b. P25 is well-known for its superior photocatalytic activity ascribed to the mixed phases (78% anatase and 22% rutile in mass fraction) and specific surface area (53 $m^2 g^{-1}$) [26]. It is also generally regarded that anatase is the more photochemically active phase of titania than rutile. However, in the present case, the 3D TiO_2 assembled with radially aligned rutile nanorods synthesized with 0.4 M TNB at 150 and 120 °C shows better or equivalent photocatalytic activity compared with P25. This enhancement of photocatalytic performance can be mainly ascribed to the high light harvesting ability realized by the unique dandelion-like morphology of 3D hierarchical structure, in which the interspaces act as the channel for light transfer and tapered tip geometry favors lower reflectance. Besides, less aggregation for this well-controlled structure also enhances high photocatalytic activity.

4. Conclusions

3D dandelion-like nanostructures composed of radially aligned rutile nanorods have been successfully synthesized by the present solvothermal method. The microstructures and properties of 3D TiO_2 microspheres can be altered by adjusting the reaction temperature and reactant concentration. When the reaction temperature is increased from 120 to 210 °C, the resultant particle size of rutile crystals is increased, but the aspect ratios of one-dimensional rutile nanocrystals reduced. Dandelion-like morphology can be obtained with TNB concentration ranging from 0.3 to 0.5 M, while lower TNB concentration (0.2 M) leads to the collapse of microspheres and sector formation. 3D dandelion-like structures with tapered tips show better photocatalytic activity than those with flat tops and nanorod sector fragment due to lower reflectance, more efficient light harvesting and higher surface area. Furthermore, TiO_2 products prepared with 0.4 M titanium precursor solution at 150 and 120 °C show better or equivalent photocatalytic activity compared with P25, which can be attributed to the efficient light harvesting and less aggregation for the well-controlled 3D dandelion-like hierarchical structure.

Acknowledgment

This work is supported by the National Natural Science Foundation of China (51172201), the Foundation of the Department of Education, Zhejiang Province, China (Y200909120) and the Fundamental Research Funds for the Central Universities, China.

References

[1] B. Oregan, M. Gratzel, A low-cost, high-efficiency solar-cell based on dye-sensitized colloidal TiO_2 films, Nature 353 (1991) 737–740.
[2] R. Asahi, T. Morikawa, T. Ohwaki, K. Aoki, Y. Taga, Visible-light photocatalysis in nitrogen-doped titanium oxides, Science 293 (2001) 269–271.
[3] M.M. Viana, V.F. Soares, N.D.S. Mohallem, Synthesis and characterization of TiO_2 nanoparticles, Ceramics International 36 (2010) 2047–2053.
[4] M.S. Liang, C.C. Khaw, C.C. Liu, S.P. Chin, J. Wang, H. Li, Synthesis and characterisation of thin-film TiO_2 dye-sensitised solar cell, Ceramics International 39 (2013) 1519–1523.
[5] F. Amano, K. Nogami, B. Ohtani, Visible light-responsive bismuth tungstate photocatalysts: effects of hierarchical architecture on photocatalytic activity, Journal of Physical Chemistry C 113 (2009) 1536–1542.
[6] D.V. Bavykin, A.N. Kulak, V.V. Shvalagin, N.S. Andryushina, O.L. Stroyuk, Photocatalytic properties of rutile nanoparticles obtained via low temperature route from titanate nanotubes, Journal of Photochemistry and Photobiology A 218 (2011) 231–238.
[7] H.G. Bang, J.K. Chung, R.Y. Jung, S.Y. Park, Effect of acetic acid in TiO_2 paste on the performance of dye-sensitized solar cells, Ceramics International 38 (2012) S511–S515.

[8] N.H.N. Yusoff, M.J. Ghazali, M.C. Isa, A.R. Daud, A. Muchtar, Effects of powder size and metallic bonding layer on corrosion behaviour of plasma-sprayed Al_2O_3–13% TiO_2 coated mild steel in fresh tropical seawater, Ceramics International 39 (2013) 2527–2533.
[9] S. Mohammadi, H. Abdizadeh, M.R. Golobostanfard, Effect of niobium doping on opto-electronic properties of sol–gel based nanostructured indium tin oxide thin films, Ceramics International 39 (2013) 4391–4398.
[10] X.L. Bal, B. Xie, N. Pan, X.P. Wang, H.Q. Wang, Novel three-dimensional dandelion-like TiO_2 structure with high photocatalytic activity, Journal of Solid State Chemistry 181 (2008) 450–456.
[11] X.X. Ren, G.L. Zhao, H. Li, W. Wu, G.R. Han, The effect of different pH modifier on formation of CdS nanoparticles, Journal of Alloys and Compounds 465 (2008) 534–539.
[12] J. Zhou, G.L. Zhao, J.J. Yang, G.R. Han, Diphenylthiocarbazone (dithizone)-assisted solvothermal synthesis and optical properties of one-dimensional CdS nanostructures, Journal of Alloys and Compounds 509 (2011) 6731–6735.
[13] Y.X. Li, Y.F. Hu, S.Q. Peng, G.X. Lu, S.B. Li, Synthesis of CdS nanorods by an ethylenediamine assisted hydrothermal method for photocatalytic hydrogen evolution, Journal of Physical Chemistry C 113 (2009) 9352–9358.
[14] J. Zhou, G.L. Zhao, B. Song, G.R. Han, Solvent-controlled synthesis of TiO_2 three-dimensional nanostructures via a one-step solvothermal route, Crystal Engineering Communications 13 (2011) 2294–2302.
[15] E. Hosono, S. Fujihara, K. Kakiuchi, H. Imai, Growth of submicrometer-scale rectangular parallelepiped rutile TiO_2 films in aqueous $TiCl_3$ solutions under hydrothermal conditions, Journal of the American Chemical Society 126 (2004) 7790–7791.
[16] T.P. Niesen, M.R. De Guire, Review: deposition of ceramic thin films at low temperatures from aqueous solutions, Journal of Electroceramics 6 (2001) 169–207.
[17] J.Q. Luo, L. Gao, Large-scale production of monodispersed titania microspheres by surfactant-guided self-assembly, Journal of Alloys and Compounds 487 (2009) 763–767.
[18] L. Liu, Y.P. Zhao, H.J. Liu, H.Z. Kou, Y.Q. Wang, Directed growth of TiO_2 nanorods into microspheres, Nanotechnology 17 (2006) 5046–5050.
[19] T. Sugimoto, X.P. Zhou, A. Muramatsu, Synthesis of uniform anatase TiO_2 nanoparticles by gel-sol method—1. Solution chemistry of Ti(OH)(n)((4−n)+) complexes, Journal of Colloid and Interface Science 252 (2002) 339–346.
[20] L. Kavan, B. Oregan, A. Kay, M. Gratzel, Preparation of Tio_2 (Anatase) films on electrodes by anodic oxidative hydrolysis of $TiCl_3$, Journal of Electroanalytical Chemistry 346 (1993) 291–307.
[21] J.G. Li, T. Ishigaki, X.D. Sun, Anatase, brookite, and rutile nanocrystals via redox reactions under mild hydrothermal conditions: phase-selective synthesis and physicochemical properties, Journal of Physical Chemistry C 111 (2007) 4969–4976.
[22] H.B. Li, X.C. Duan, G.C. Liu, X.B. Jia, X.Q. Liu, Morphology controllable synthesis of TiO_2 by a facile hydrothermal process, Materials Letters 62 (2008) 4035–4037.
[23] G.H. Tian, Y.J. Chen, W. Zhou, K. Pan, C.G. Tian, X.R. Huang, et al., 3D hierarchical flower-like TiO(2) nanostructure: morphology control and its photocatalytic property, Crystal Engineering Communications 13 (2011) 2994–3000.
[24] L.K. Yeh, K.Y. Lai, G.J. Lin, P.H. Fu, H.C. Chang, C.A. Lin, et al., Giant efficiency enhancement of GaAs solar cells with graded antireflection layers based on syringelike ZnO nanorod arrays, Advanced Energy Materials 1 (2011) 506–510.
[25] S.L. Diedenhofen, G. Vecchi, R.E. Algra, A. Hartsuiker, O.L. Muskens, G. Immink, et al., Broad-band and omnidirectional antireflection coatings based on semiconductor nanorods, Advanced Materials 21 (2009) 973–978.
[26] J.G. Yu, Y.R. Su, B. Cheng, Template-free fabrication and enhanced photocatalytic activity of hierarchical macro-/mesoporous titania, Advanced Functional Materials 17 (2007) 1984–1990.